

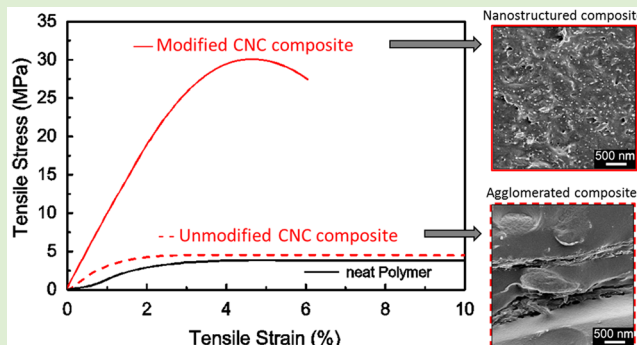
Strong Surface Treatment Effects on Reinforcement Efficiency in Biocomposites Based on Cellulose Nanocrystals in Poly(vinyl acetate) Matrix

Farhan Ansari,[†] Michaela Salajková,^{†,‡} Qi Zhou,^{‡,§} and Lars A. Berglund^{*,†,‡}

[†]Department of Fiber and Polymer Technology and [‡]Wallenberg Wood Science Center, KTH Royal Institute of Technology, SE-100 44 Stockholm, Sweden

[§]School of Biotechnology, Royal Institute of Technology, AlbaNova University Centre, SE-106 91 Stockholm, Sweden

ABSTRACT: In this work, the problem to disperse cellulose nanocrystals (CNC) in hydrophobic polymer matrices has been addressed through application of an environmentally friendly chemical modification approach inspired by clay chemistry. The objective is to compare the effects of unmodified CNC and modified CNC (modCNC) reinforcement, where degree of CNC dispersion is of interest. Hydrophobic functionalization made it possible to disperse wood-based modCNC in organic solvent and cast well-dispersed nanocomposite films of poly(vinyl acetate) (PVAc) with 1–20 wt % CNC. Composite films were studied by infrared spectroscopy (FT-IR), UV-vis spectroscopy, dynamic mechanical thermal analysis (DMTA), tensile testing, and field-emission scanning electron microscopy (FE-SEM). Strongly increased mechanical properties were observed for modCNC nanocomposites. The reinforcement efficiency was much lower in unmodified CNC composites, and specific mechanisms causing the differences are discussed.



INTRODUCTION

Cellulose is the main load bearing component of plant cell walls and is present in the form of microfibrils. The microfibrils (plant physiology term) are nanofibers with lateral dimensions typically in the range of 3–10 nm, depending on the plant origin, and lengths of at least 1 μm . The cellulose molecules are in extended chain conformation with strong secondary inter- and intramolecular interactions between molecules in the cellulose crystallites. As a consequence, strength and modulus of fibrous cellulose can be very high in the axial direction of the molecules.^{1,2} Favier and colleagues demonstrated that elastomeric polymer matrix composites based on acid-hydrolyzed cellulose nanorods can show strong modulus enhancement at a reinforcement content of just a few percent.^{3,4} This inspired widespread research efforts on cellulose nanocomposites. In the early 1950s, Battista⁵ found that rod-like particles can be isolated from cellulose by hydrochloric acid hydrolysis. The acid degraded the molecularly disordered regions in cellulose microfibrils so that rod-like particles of nanoscale dimensions were obtained.⁵ This type of nanoscale cellulose is termed microcrystalline cellulose and is widely used commercially, for instance, as a binder in tablets for pharmaceutical use.⁶ Smaller diameter cellulose nanocrystals (CNC) can be prepared by cellulose hydrolysis with sulfuric acid, as was first discovered by Rånby et al.⁷ CNC shows very interesting chiral nematic behavior in colloidal suspension and this phenomenon has been studied thoroughly.^{8–10} In contrast to hydrochloric acid

hydrolysis, the sulfuric acid method results in colloidal suspensions of CNC where the nanoparticles are stabilized by electrostatic repulsion of negatively charged sulfate ester groups at the CNC surface. If followed by cationization,¹¹ the suspension is stabilized by positively charged groups. Recently, phosphoric acid¹² or mildly acidic aqueous ionic liquids¹³ have been used to isolate CNC.

One limitation with CNC as a reinforcement is that it is quite hydrophilic and therefore most commonly used with hydrophilic and water-soluble polymer matrices. CNC is easy to mix with hydrophilic polymers, and strong adhesion can be obtained at the CNC/polymer interface. In order to broaden the range of polymers available for successful CNC-reinforcement beyond water-soluble materials, surface modification of CNC can be used.^{14,15} Generally, surface modification of cellulose includes either covalent modification such as esterification,^{16,17} silylation,¹⁸ polymer grafting,^{19–21} or non-covalent modification using polyelectrolytes^{22,23} or surfactants.^{24–29}

Surfactants enable simple, fast, and efficient methods for surface modification of cellulose nanocrystals. Heux et al.²⁵ showed that anionic surfactant (phosphoric ester of polyoxyethylene nonylphenyl ether) modified CNCs can form stable

Received: September 15, 2015

Revised: October 17, 2015

Published: October 27, 2015

dispersions and show chiral nematic phase formation in cyclohexane. Later on, the same surfactant was used to prepare nanocomposites with PLA either by solution casting^{26,28} or by extrusion.²⁴ In all cases, the surfactant significantly improved the dispersion of CNC in the comparably hydrophobic PLA matrix. Recently, the same approach was used to produce ternary composites with PLA, CNC, and silver nanoparticles.³⁰ Moreover, Ljungberg et al.²⁷ compared performance of surfactant-modified CNC and maleated polypropylene grafted whiskers in atactic polypropylene matrix (aPP). The surfactant provided better dispersion of CNC in the aPP matrix than grafting, resulting in materials with better mechanical properties.

In a previous study, a “green” approach to surface modification of CNC was developed.²⁹ Hydrophobic hydrocarbon surfactants could simply be attached to the CNC surface in environmentally friendly water suspensions. The attachment mechanism was through ionic interactions between the charged groups on the CNC and the ammonium group at one end of the hydrocarbon surfactant. The remaining part of the surfactant molecule consisted of a short linear and hydrophobic hydrocarbon chain. This method was inspired by an approach used in clay chemistry. The present objective is to study the effect of such hydrophobically functionalized CNCs on the quality of dispersion of CNC in a more hydrophobic polymer matrix. Poly(vinylacetate) (PVAc) is used as a polymer matrix model. Well-dispersed and truly nanostructured biocomposites based on surface-treated CNC and PVAc are prepared and the effects of surface treatment on dispersion, glass transition temperature (T_g), and mechanical properties are investigated. The surface treatment procedure could also be used for CNC/PVAc adhesives or composites mixed by melt compounding.

EXPERIMENTAL SECTION

Materials. Dissolving softwood pulp with high cellulose content (ca. 93%) was kindly supplied by Domsjö Fabriker AB. Polyvinyl acetate ($M_w = 83000$) was obtained from Aldrich in the form of pellets. Sulfuric acid (Analytical Reagent grade, Fisher Scientific), sodium hydroxide (Reagent grade, Sigma-Aldrich), dodecyltrimethylammonium chloride (Puriss, Aldrich), toluene (ACS, Reagent Ph Eur, Merck), and uranyl acetate dehydrate (>98%, Fluka) were used without further purification.

Preparation of Cellulose Nanocrystals. Cellulose nanocrystals were prepared from wood pulp using sulfuric acid hydrolysis according to method described by Beck-Candanedo¹⁰ with minor modifications. Briefly, 20 g of dry wood pulp was cut using a kitchen blender (Nordica OBH) and added to 175 mL of 64 wt % sulfuric acid preheated to 45 °C. The reaction was kept at 45 °C for 60 min and afterward diluted to 10% of the original concentration in order to stop the reaction. The suspension was centrifuged at 4754 g for 15 min (Rottina 420, Hettich Centrifuge), washed with water, and re-centrifuged. The remaining acid was washed for several days with dialysis using Spectrum Spectra/Por regenerated cellulose dialysis membranes with a molecular weight cutoff of 12 000–14 000 for several days, until the pH of the surrounding water was neutral. The resulting suspension of cellulose nanocrystals was sonicated for 2 × 5 min at 50% of maximum power using an Ultrasonic processor (Sonics Vibracell, VCX 750, Sonic&Materials, U.S.A.) equipped with a 3 mm tip. The suspension was then purified by centrifugation at 4754 g for 60 min, and the concentration, as determined by gravimetric analysis, was 1.1 wt %. The surface charge was determined by conductometric titration and was 0.5 mmol/g.

Hydrophobization of Cellulose Nanocrystals. The surface of the CNC was modified according to a procedure previously developed in our laboratory, with minor modifications.²⁹ The pH of the CNC suspension was adjusted to 10 using a sodium hydroxide solution and

the final concentration was 1 wt %. Afterward, dodecyltrimethylammonium chloride (DTAC or C12) was added at four different contents corresponding to the molar ratios between sulfate ester groups present on the surface of the CNC and the C12 (1:2, 1:4, 1:8, and 1:16). This was in order to optimize the amount of C12 required for successful redispersion of C12 modified CNC in toluene. The suspensions were therefore stirred overnight, freeze-dried, and redispersed in toluene. The modCNC suspension in toluene was centrifuged at 12100 g (Eppendorf) to remove excess C12. It was then redispersed in fresh toluene, and the concentration was adjusted to 1 wt % with respect to pure cellulose. The optimal ratio was found to be 1:4 and this ratio was used for further experiments. A suspension of 1 wt % unmodified CNC (pH = 10) was freeze-dried and redispersed in a suspension of toluene and used as a control.

Characterization of Hydrophobized CNC. The modification of CNC with C12 was confirmed by FT-IR. The spectra were recorded using PerkinElmer Spectrum 2000 FTIR equipped with a MKII Golden Gate, single reflection attenuated total reflectance (ATR) system (Specac Ltd, London, UK). The ATR crystal was a MKII heated diamond 45 ATR top plate.

The transparency of the modCNC suspensions in toluene was evaluated by UV-vis spectrophotometry (UV-2550 UV-vis spectrophotometer, Shimadzu). The transmittance spectrum was recorded between 200 and 800 nm.

The morphology of unmodified and C12 modified CNC was studied by transmission electron microscopy. A diluted suspension (0.005 wt %) was deposited on a copper grid (Ultrathin Carbon Type-A, Ted pella) for water-based suspension or Ultrathin Carbon Film on Lacey Carbon Support Film (Ted Pella) for toluene-based suspension, stained with fresh 2 wt % uranyl acetate solution, and visualized using a transmission electron microscope (Hitachi HT-7700, Japan) operated at 80 kV.

Preparation of CNC/PVAc Nanocomposite. Nanocomposites containing 1, 3, 5, 10, and 20 wt % of C12 modified CNC as well as unmodified CNC were prepared. The desired amount of CNC was dispersed in 10 mL of toluene by sonication for 30 s using the Ultrasonic disintegrator equipped with a 3 mm microtip at 30% maximum power. Afterward, PVAc was added and the total weight of the nanocomposite was fixed to be 1 g. The suspensions were stirred overnight to ensure complete dissolution of PVAc. The suspension was cast in an aluminum Petri dish and dried at room temperature for a week and further at 60 °C for 5 days.

Characterization of CNC/PVAc Nanocomposites. The transparency of the nanocomposite films was studied using UV-vis spectrophotometry. A piece of the film was placed over the cuvette holder and the transmittance spectrum was recorded between 200 and 800 nm.

The mechanical properties of the films were tested using Instron 5944 instrument equipped with a 500 N load cell. The samples were cut into rectangular strips, 5 mm wide and 0.2 mm thick. The gap between the clamps was 30 mm and the test speed was 50%/min. The samples were conditioned at 23 °C and 50% relative humidity for 2 days prior to testing. For increased accuracy in determining the elastic modulus, strain in the initial elastic region (up to 0.2%) was measured using 2D Differential Speckle Photography (DSP). Black paint was sprayed on the samples, resulting in a uniform, fine pattern. Correlation was done using the LIMESS software.

Dynamic Mechanical Thermal Analysis (DMTA) was done using a TA Instruments Q800 in tensile mode on rectangular samples (4 mm by 10 mm). Measurements were taken at a frequency of 1 Hz and an amplitude of 10 μm. The temperature scan was performed between –20 and 120 °C at a rate of 5 °C/min. The glass transition temperature was determined from the loss modulus peak.

The morphology and the degree of dispersion of unmodified and C12 modified CNC in PVAc matrix was studied using Field Emission Scanning Electron Microscope (FE-SEM, Hitachi S-4800, Hitachi, Japan). The cross section of the samples was prepared by fracture under liquid nitrogen. The samples were attached on a split mount stub using carbon tape and coated with a thin layer of Pt/Pd (Cressington 208 sputter coater).

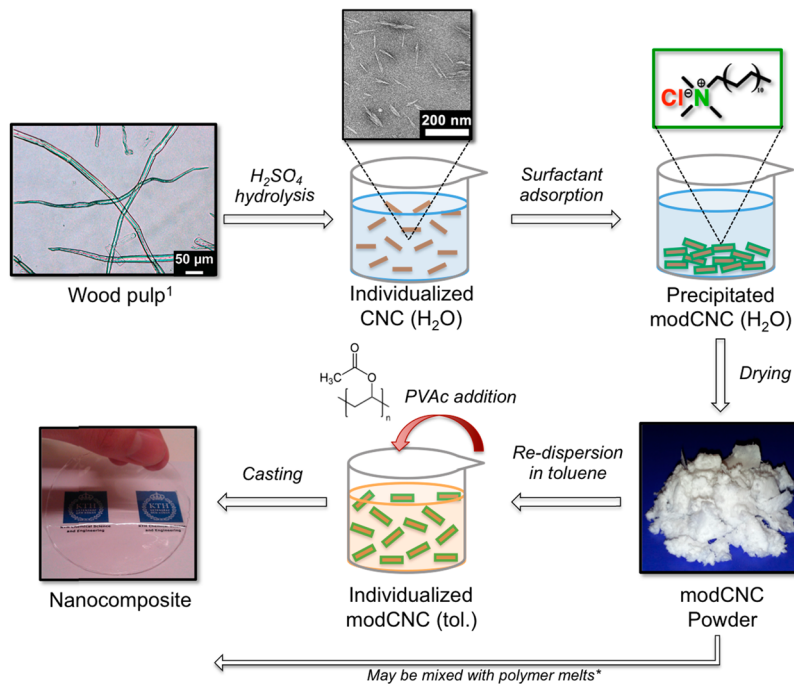


Figure 1. Schematic illustration of nanocomposite preparation: isolation of CNC from wood pulp by sulfuric acid hydrolysis and surface modification with dodecyltrimethylammonium chloride (C12) in aqueous suspension followed by freeze-drying and redispersion in toluene, addition of PVAc and removal of the solvent by casting to form the nanocomposite. (*This arrow represents the potential to mix modified CNC with liquid monomers or thermoplastic melts.¹ The wood pulp image is reprinted with permission from Saito et al.³⁶ Copyright 2007 American Chemical Society). The KTH logo is used with permission from Royal Institute of Technology (KTH), Sweden.

Micromechanics Model. Composite modulus was predicted by an empirical combination (eq 1) of the longitudinal modulus (rule of mixtures, see eq 2) and transverse modulus (Halpin–Tsai equations, see eqs 3 and 4). This model was developed to predict the modulus of random-in-plane short fiber composites with cylindrical fibers.^{31,32}

$$E_C = \frac{3}{8}E_L + \frac{5}{8}E_T \quad (1)$$

where

$$E_L = E_{f,t} \cdot V_f + E_m \cdot (1 - V_f) \quad (2)$$

$$E_T = E_m \left(\frac{1 + 2 \cdot \eta \cdot V_f}{1 - \eta \cdot V_f} \right) \quad (3)$$

$$\eta = \frac{(E_{f,t} - E_m)}{(E_{f,t} + 2E_m)} \quad (4)$$

In the above equations, V_f and V_m represent the volume fraction of CNC and matrix, respectively (weight fractions were converted to volume fractions using a relative density of 1.5 for CNC and 1.18 for PVAc); E_C , E_m , $E_{f,l}$, $E_{f,t}$ represent the composite modulus, matrix modulus, longitudinal CNC modulus, and transverse CNC modulus, respectively. The values of longitudinal ($E_{f,l} = 105$ GPa) and transverse ($E_{f,t} = 15$ GPa) CNC modulus were taken from literature.^{33,34}

RESULTS AND DISCUSSION

CNC Characterization. CNC was prepared by sulfuric acid hydrolysis of wood pulp (Figure 1), so that a hydrocolloidal suspension of rod-like nanoparticles was obtained. The CNC nanoparticles were approximately 100–300 nm in length and 3–5 nm wide as estimated from the TEM images (Figure 2d). The CNC was stabilized in the suspension via electrostatic repulsion due to the sulfate ester groups introduced during the

hydrolysis.^{7,8} The charge of the CNC was 0.5 mmol/g, as determined by conductometric titration.

Afterward, CNC was modified with dodecyltrimethylammonium chloride (C12, Figure 1) using a method previously developed by Salajkova et al.²⁹ In order to optimize the reaction conditions, four different molar ratios between CNC sulfate ester groups and C12 were chosen (1:2, 1:4, 1:8, and 1:16). The adsorption was successful in all cases as confirmed by FT-IR (Figure 2a). New peaks were observed at 2900 and 2850 cm⁻¹, corresponding to asymmetrical and symmetrical CH₂ stretches from the long alkyl chain of dodecyltrimethylammonium chloride.³⁵ The intensity of the peak becomes stronger with decreasing CNC/C12 ratio.

In the present study, the previous procedure was modified so that the aqueous CNC suspension was used at higher concentration (1 wt %) using direct addition of C12 surfactant powder rather than mixing with a liquid surfactant suspension (see Experimental Section). The amount of water removed during freeze-drying was thus reduced to less than 1/15th of the amount used in the previous study.²⁹ This reduces the energy consumption of the process significantly and increases the potential for up-scaling. Freeze-drying of the modCNC also makes it possible to use a powder of modCNC in melt mixing.

The freeze-dried nanocrystals were dispersed in toluene (Figure 1) and the quality of the dispersions of the CNCs modified with different CNC/C12 ratios was studied using UV-vis spectrophotometry (Figure 2b). The unmodified CNC in water was used as a reference and showed very high transmittance. It was not possible to obtain reliable data for unmodified CNC in toluene and modCNC 1:2 due to the presence of agglomerates (Figure 2c). For C12-modified CNC with CNC/C12 ratios of 1:4, 1:8, and 1:16 it was possible to obtain stable suspensions in toluene (Figure 2b), but the

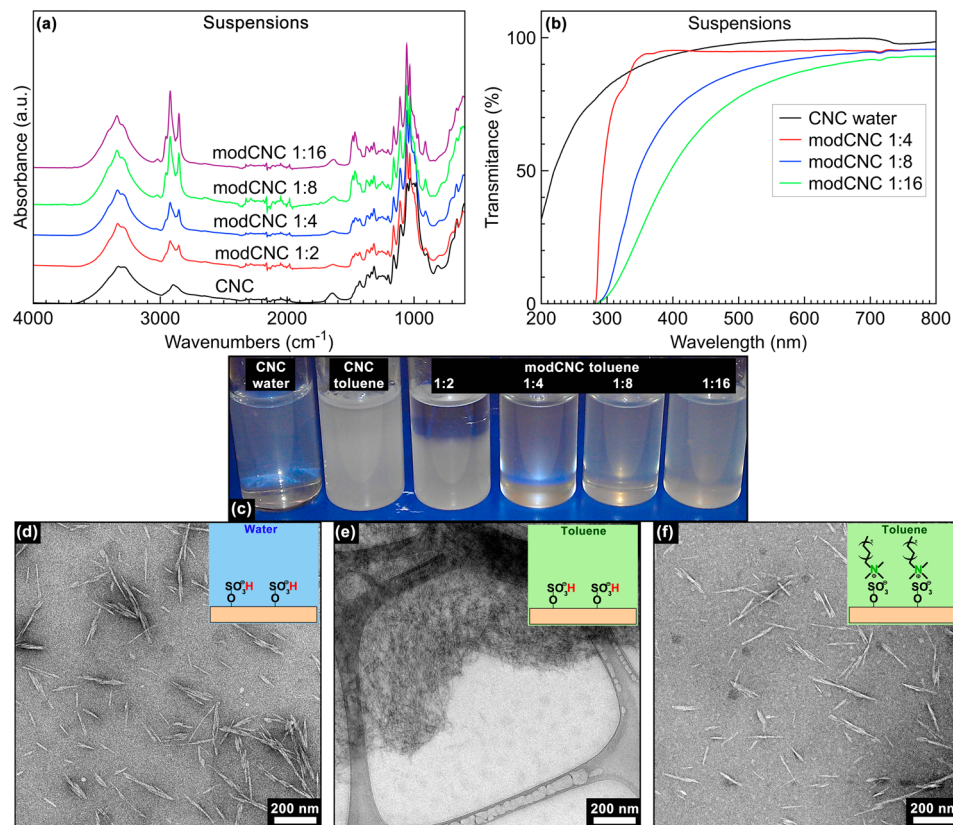


Figure 2. (a) FT-IR spectra of unmodified and C12 modified CNC (note the different CNC/C12 ratios), (b) UV-vis spectra of unmodified CNC in water and C12-modified CNC in toluene (note the different CNC/C12 ratios), (c) photography of CNC suspensions, left to right: unmodified CNC in water, unmodified CNC in toluene, C12-modified CNC with different ratios CNC/C12, 1:2, 1:4, 1:8 and 1:16, (d) TEM image of unmodified CNC dried from water, (e) TEM image of unmodified CNC dried from toluene, and (f) TEM image of C12 modified CNC (ratio 1:4) dried from toluene.

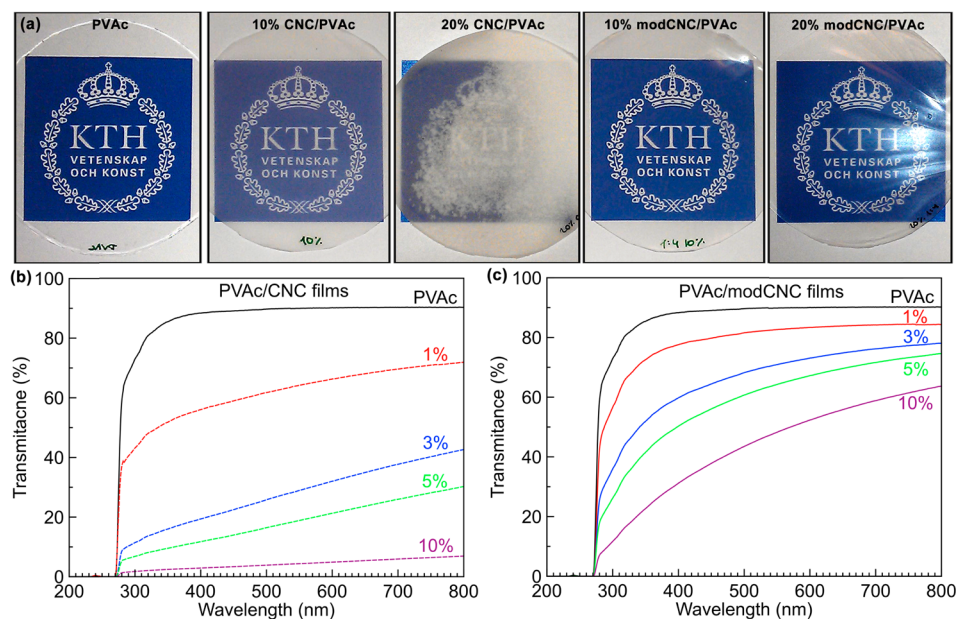


Figure 3. (a) Photographs of films obtained by solvent casting of (left to right) pure PVAc, 10 wt % CNC/PVAc, 20 wt % CNC/PVAc, 10 wt % modCNC/PVAc, and 20 wt % modCNC/PVAc, (b) UV-vis spectra of nanocomposites with unmodified CNC/PVAc, and (c) C12-modified CNC/PVAc. The KTH logo is used with permission from Royal Institute of Technology (KTH), Sweden.

transmittance decreased with increasing amount of C12. Possibly, the reason is formation of C12 micelles at higher CNC/C12 ratios.^{37,38} It was concluded that a CNC/C12 ratio

of 1:4 provided a stable suspension with high transmittance using the least amount of C12. This ratio was therefore chosen for further experiments.

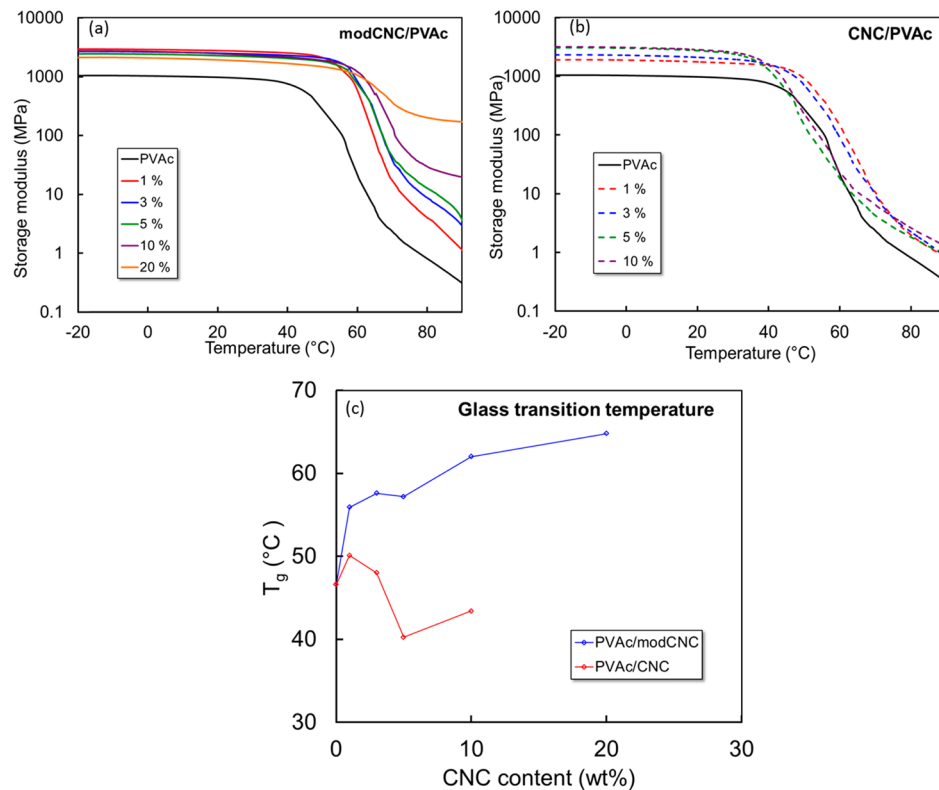


Figure 4. DMTA curves for PVAc nanocomposites containing (a) modified CNC, (b) unmodCNC, and (c) the T_g as a function of cellulose content for modCNC/PVAc and CNC/PVAc nanocomposites.

The morphology of the CNC suspensions was studied using TEM. Both unmodified CNC in water suspension (**Figure 2d**) and modCNC 1:4 in toluene (**Figure 2f**) showed well-individualized nanoparticles without large agglomerates, whereas unmodified CNC in toluene showed large agglomerates at the micrometer scale (**Figure 2e**).

Since one goal of the present study is to prepare biocomposites with well-dispersed CNC nanoparticles, the importance of a stable and well-dispersed liquid suspension as a starting point cannot be exaggerated. Many nanocomposites studies in the literature are on agglomerated systems where the properties are not improved to the full potential. In the present study, the importance of good dispersion and a favorable CNC/PVAc interface is clarified.

CNC nanocomposites with PVAc matrix were prepared by mixing PVAc and CNC in toluene (**Figure 1**), followed by solvent casting (**Figure 1**). A series of samples, with CNC content of 1–20 wt % was prepared using both C12 modified CNC (1:4) and unmodified CNC (**Figure 3a**). CNC/PVAc nanocomposites were translucent with significantly reduced transmittance (**Figure 3b**). ModCNC/PVAc nanocomposites were homogeneous and transparent, with transmittance above 50% at a CNC content of 1–10 wt % (**Figure 3c**). However, the composite containing 20 wt % unmodified CNC was not homogeneous and showed distinct regions of phase separation of CNC from the PVAc matrix (**Figure 3a**). The reason is simply that unmodified CNC and PVAc are not compatible. Due to the inhomogeneity of the 20% unmodified CNC/PVAc composite, it was not further characterized.

Composite Characterization. The properties of PVAc films can differ significantly depending on moisture content,^{39–41} molecular weight, side group branching, preparation

method, and so on. For example, films prepared by solvent casting show much lower strength and modulus than thermally processed PVAc materials,⁴² possibly due to higher free volume in PVAc prepared by solvent casting. The phenomenon of physical aging has been studied in PVAc.^{43,44} To avoid uncontrolled aging effects, all mechanical property characterization tests were performed directly after conditioning the films at 23 °C and 50% RH for 2 days.

The temperature-dependence of mechanical properties was studied using DMTA. The storage modulus was plotted against temperature for composites with unmodified (**Figure 4a**) and modified (**Figure 4b**) cellulose. As is apparent from **Figure 4**, the onset of the glass transition is shifted to higher temperatures for modCNC/PVAc composites, while the shift was negligible (or very small) for the unmodified CNC/PVAc composites. It is also interesting to note that modCNC/PVAc composites with high modCNC content exhibited a much higher and rather stable modulus at temperatures above the glass transition. The T_g values were calculated from the position of the loss modulus peak and are reported in **Figure 4c** and **Table 1**. In case of the composites with unmodified CNC, the T_g increased by about 3 °C on adding 1 wt % CNC and thereafter decreased somewhat with increasing CNC content. On the other hand, the T_g increase for composites containing C12-modified CNC (**Figure 4c**) was rather large. Addition of only 1 wt % of modCNC led to almost 9 °C increase in T_g . This increased further with increasing modCNC content (ca., 18 °C increase with 20 wt % modCNC). The mobility of the PVAc molecules close to the CNC nanoparticles is restricted by the CNC, so that the T_g is shifted to higher temperatures. Physical aging of PVAc promoted by the modCNC is an important part of the effect, as will be discussed.

Table 1. T_g Data for CNC/PVAc and modCNC/PVAc Nanocomposites, as Determined by DMTA

CNC content (wt %)	CNC/PVAc	modCNC/PVAc
	T_g (°C)	T_g (°C)
0	47	47
1	50	56
3	48	56
5	40	57
10	43	62
20		65

Similar results were observed by Keddie et al.,⁴⁵ where an increase in T_g of PMMA on a silicon substrate was explained as a result of restricted mobility of polymer chains due to hydrogen bonding with the silicone surface. In reactive polymer systems, effects of nanocellulose on polymer matrix T_g can be even larger since the cross-link density is influenced by the presence of functional groups on the cellulose surface.^{46–48}

Mechanical properties of the nanocomposites were also studied using uniaxial tensile tests. Typical stress-strain curves for CNC/PVAc and modCNC/PVAc composites are shown in Figure 5a and b, respectively. The tensile strength as well as the modulus increase dramatically as small amounts of modCNC are added (Figure 5b). The modulus increased from 0.24 to 0.92 GPa and strength from 4.6 to 15 MPa as 1 wt % modCNC is added. The addition of unmodified CNC also had a positive effect on strength and modulus, but the increase was much lower. A comparison of maximum reinforcement between modified and unmodified CNC composite (Table 2) reveals that the strength was about 6× higher in modCNC/PVAc composites compared with neat PVAc, while it was only 1.5× higher in CNC/PVAc.

Furthermore, the maximum in strength versus CNC content is reached at 3 wt % for unmodified CNC/PVAc, while for modCNC/PVAc the strength maximum is at 10 wt % CNC content, see Figure 5d. The unmodified CNC particles start to form agglomerates at lower CNC content. The agglomerates lead to stress concentrations so that failure occurs at lower stress. However, agglomeration is a problem for modCNC/PVAc also. Beyond 5 wt % modCNC, there is no improvement in modulus (E) for modCNC/PVAc, see Figure 5c.

The reinforcement effects from modCNC are so dramatic (see Table 2 and Figure 5) that they cannot be explained by modCNC reinforcement alone. The properties of the matrix itself must also be improved by interaction with well-dispersed modCNC; otherwise, the strong improvements demonstrated in Figure 5 are unlikely. The modCNC nanoparticles may induce rapid physical aging in the PVAc matrix. Physical aging takes place in glassy polymers, where the molecular conformations of bulk polymer molecules are not in thermodynamic equilibrium.⁴⁹ The polymer undergoes slow reorganization, which is temperature-dependent, toward a more stable and dense structure. Polymers subjected to physical aging show reduced free volume, increased density, increased glassy state modulus, and may become more brittle.^{49,50}

Previous work has demonstrated that inorganic nanoparticles can accelerate the rate of aging in polymer matrix nanocomposites due to interactions with the polymer matrix.^{50–52} A high interface area is essential in accelerating physical aging.^{50,52} The mechanism involves diffusion of free volume holes, and the ratio between interfacial area and polymer volume is an essential parameter in the theoretical model.⁵² As a consequence, small and well-dispersed particles of high volume fraction would provide the strongest physical aging effects. Bujans et al. observed that the time to reach the plateau for

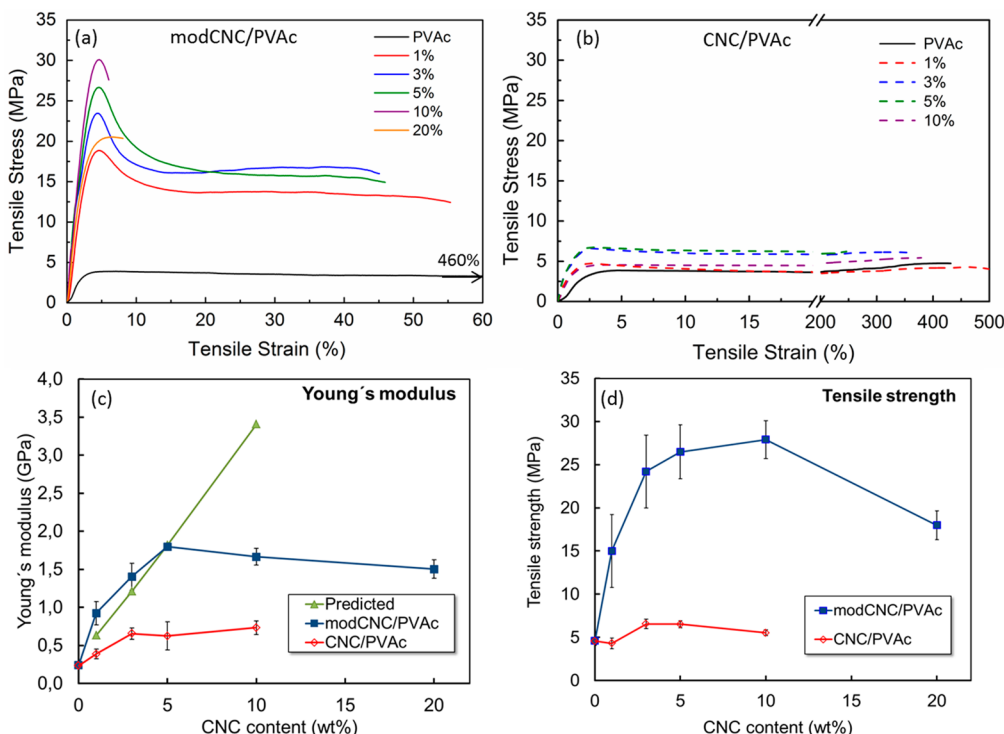


Figure 5. Typical stress-strain curves for (a) modCNC/PVAc nanocomposites and (b) unmodCNC/PVAc composites, (c) Young's modulus, and (d) the tensile strength for CNC/PVAc and modCNC/PVAc as a function of cellulose nanocrystal content.

Table 2. Average Mechanical Properties Derived from Stress–Strain Curves Obtained During Uniaxial Tensile Tests^a

CNC content		CNC/PVAc			modCNC/PVAc			Young's modulus predicted ^b (GPa)
wt %	vol %	Young's modulus (GPa)	ultimate tensile strength (MPa)	strain to failure (%)	Young's modulus (GPa)	ultimate tensile strength (MPa)	strain to failure (%)	
0	0	0.24 (0.03)	4.6 (0.5)	460 (31)	0.24 (0.03)	4.6 (0.5)	460 (31)	
1	0.8	0.39 (0.06)	4.3 (0.6)	500 (11)	0.92 (0.16)	15 (4.2)	46 (13)	0.63
3	2.4	0.65 (0.07)	6.6 (0.4)	420 (52)	1.40 (0.18)	22 (2.2)	50 (13)	1.21
5	4.0	0.63 (0.19)	6.5 (0.6)	350 (82)	1.80 (0.04)	25 (2.1)	42 (3.6)	1.82
10	8.0	0.73 (0.09)	5.5 (0.3)	400 (17)	1.66 (0.11)	28 (2.1)	5.2 (0.8)	3.41
20	16				1.50 (0.12)	18 (1.7)	4.6 (1)	6.62

^aThe values in brackets are standard deviations. ^bSee eqs 1–4.

enthalpy recovery (signifying an equilibrium state) was reduced from more than a month for neat polystyrene to just 1 day when 0.5 wt % of functionalized graphene was added to the matrix.⁵³ In the present work, the presence of high surface area nanocellulose and corresponding modCNC–PVAc interactions significantly accelerate physical aging. It is quite interesting that a CNC polymer nanoparticle can stimulate such a strong effect. The phenomenon is apparently not restricted to inorganic nanoparticles.

The reinforcement of PVAc due to modCNC nanoparticles is based on two effects. The first is due to established reinforcement mechanisms from stiff particles in a soft matrix, which can be described by micromechanics models.³¹ At higher CNC contents, agglomeration effects reduce the effective aspect ratio of the particles and modulus is much reduced, as is apparent from the trend in Figure 5c. The most dramatic reinforcement effect is, obviously, the strong increase in strength and modulus between neat PVAc and modCNC/PVAc with only 1 wt % modCNC. Here the second reinforcement effect dominates, which is increased modulus of the PVAc due to physical aging induced by the modCNC particles. Theoretical predictions by an established model show weaker reinforcement effects (predicted modulus) than experimentally observed, at least up to 3 wt % CNC in modCNC/PVAc composite (see Table 2 and Figure 5c). The observation that the experimental modulus is higher than the predicted modulus is in support of modCNC particles playing a role in enhancing the matrix properties by accelerating physical aging. This effect is also apparent in Figure 4a, where thermal softening is shifted to much higher temperature as 1 wt % of modCNC is added to PVAc. Note that the time scale of the tensile test is important. The glassy to rubbery behavior transition is close to the test temperature at this test rate so that changes in T_g due to aging show strong effects on measured properties.

Cross sections of the nanocomposites were studied using FE-SEM. The films were fractured in bending after cooling in liquid nitrogen. Neat PVAc as well as nanocomposites containing 10 wt % of cellulose were studied. Neat PVAc film showed a smooth and featureless cross-section. PVAc nanocomposites with 10 wt % of unmodified CNC (Figure 6a,b) showed regions with large agglomerates of CNC (rough regions) and smooth regions rich in neat PVAc. On the other hand, nanocomposites with 10 wt % modified CNC (Figure 6c,d) showed much more homogeneous cross sections with rather individualized CNC uniformly dispersed in the PVAc matrix. The cross section in Figure 6c appears rather smooth, indicating that micron scale flocculates were not present in the composites. In the higher resolution image (Figure 6d), the

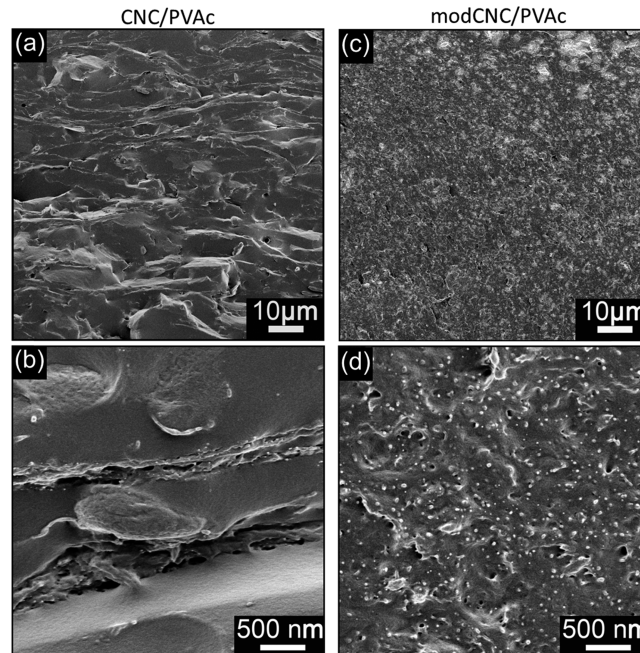


Figure 6. SEM images of cross sections of (a, b) nanocomposite containing 10 wt % unmodified CNC and (c, d) nanocomposite with 10 wt % modified CNC.

modCNC particles are apparent as white dots. Modification of CNC with C12 significantly improves mutual compatibility between otherwise hydrophilic CNC and hydrophobic PVAc. The degree of dispersion has significant effect on T_g and on the properties of the composite.

In previous work, cellulose nanofibers (CNF) and CNC were used as reinforcement for PVAc in melt compounded nanocomposites.^{41,54,55} Effects of processing conditions on physical properties have also been studied.⁵⁶ The present reinforcement effects are much stronger than in previous studies, partly due to better dispersion of the modCNC. One may note that the neat PVAc in the present study shows low modulus (0.24 GPa as compared to ~1.7 GPa in melt processed composites), and this contributes to the strong reinforcement effect. The present PVAc films are prone to physical aging since they contain high free volume due to the solvent casting procedure. Residual solvent⁵⁷ did not influence the results due to careful drying, so this artifact can be excluded. To showcase the extent of physical aging, properties of hot pressed PVAc pellets were compared after (1) quenching (rapid cooling) and (2) cooling slowly (@ 6–8 °C/hour). The quenched films had a modulus of 0.21 GPa, whereas the

modulus of the slowly cooled film was 0.92 GPa. This is in support of high free volume in solvent cast films since the modulus of quenched film is similar to the modulus of solvent cast neat PVAc. Another observation in support of physical aging is that DSC scans of modCNC/PVAc composites showed characteristic enthalpy peaks, which are associated with physically aged materials.^{50,52}

CONCLUSIONS

An environmentally friendly approach for clay-inspired surface modification of CNC nanoparticles in water was applied to prepare nanocomposites based on PVAc, a widely used polymer for ductile adhesives. The optimum ratio between CNC and a hydrophobic surfactant was determined, and the successful reactions were confirmed by FT-IR. The modCNC was successfully dispersed in organic solvent as well as in the solvent cast nanocomposite films. It was possible to add as much as 20 wt % of CNC to PVAc. There were dramatic property differences between nanocomposites based on unmodified and modified CNC. Optical transmittance was much better in modCNC composites, indicating better dispersion and fewer large agglomerates. The T_g of modCNC/PVAc material was strongly increased. This indicates strong molecular interactions between modCNC and the PVAc molecules. For instance, the polymer modulus increased from 240 to 920 MPa as 1 wt % modCNC was added, and this cannot be explained by high CNC modulus only. Good dispersion and high specific CNC/modCNC interface area resulted in rapid physical aging of PVAc and increased matrix modulus. The dynamics of the PVAc glass transition becomes more constrained and free volume decreases due to the CNC. In contrast, the unmodified CNC resulted in modest increase in modulus and strength due to agglomeration effects. Also, ultimate strength was much higher in modCNC nanocomposites, since yielding occurred at increased stress. This is due to a combination of the load-carrying ability of the stiff modCNC nanorod reinforcement and accelerated physical PVAc aging, which increased PVAc yield strength. CNC contents of 10 wt % and lower showed the strongest reinforcement effects. At higher CNC content, the degree of dispersion is compromised.

In conclusion, the potential for CNC reinforcement of ductile and fairly hydrophobic thermoplastics has been demonstrated. It is critical to obtain successful dispersion in the polymer matrix, as was demonstrated. An important target for future studies is to reach strong reinforcement effects and preserved ductility at even higher CNC content, where higher degree of dispersion is the key.

AUTHOR INFORMATION

Corresponding Author

*E-mail: blund@kth.se. Tel.: +46 8 7908118. Fax: +46 8 207865.

Notes

The authors declare no competing financial interest.

ACKNOWLEDGMENTS

Authors gratefully acknowledge funding from Knut and Alice Wallenberg foundation through Wallenberg Wood Science Center and from VINNOVA through BiMaC Innovation Excellence Centre.

REFERENCES

- (1) Isogai, A.; Saito, T.; Fukuzumi, H. TEMPO-oxidized cellulose nanofibers. *Nanoscale* **2011**, *3*, 71–85.
- (2) Sakurada, I.; Nukushina, Y. Experimental determination of the elastic modulus of crystalline regions in oriented polymers. *J. Polym. Sci.* **1962**, *57*, 651–659.
- (3) Favier, V.; Canova, G. R.; Cavaille, J. Y.; Chanzy, H.; Dufresne, A.; Gauthier, C. Nanocomposite Materials from Latex and Cellulose Whiskers. *Polym. Adv. Technol.* **1995**, *6*, 351–355.
- (4) Favier, V.; Chanzy, H.; Cavaille, J. Y. Polymer Nanocomposites Reinforced by Cellulose Whiskers. *Macromolecules* **1995**, *28*, 6365–6367.
- (5) Battista, O. A. Hydrolysis and Crystallization of Cellulose. *Ind. Eng. Chem.* **1950**, *42*, 502–507.
- (6) Battista, O. A. *Microcrystal Polymer Science*; McGraw Hill Inc.: New York, 1975.
- (7) Rånby, B. G. Fibrous macromolecular systems. Cellulose and muscles. The colloidal properties of cellulose micelles. *Discuss. Faraday Soc.* **1951**, *11*, 158–164.
- (8) Revol, J. F.; Bradford, H.; Giasson, J.; Marchessault, R. H.; Gray, D. G. Helicoidal Self-Ordering of Cellulose Microfibrils in Aqueous Suspension. *Int. J. Biol. Macromol.* **1992**, *14*, 170–172.
- (9) Dong, X. M.; Kimura, T.; Revol, J. F.; Gray, D. G. Effects of ionic strength on the isotropic-chiral nematic phase transition of suspensions of cellulose crystallites. *Langmuir* **1996**, *12*, 2076–2082.
- (10) Beck-Candanedo, S.; Roman, M.; Gray, D. G. Effect of reaction conditions on the properties and behavior of wood cellulose nanocrystal suspensions. *Biomacromolecules* **2005**, *6*, 1048–1054.
- (11) Hasani, M.; Cranston, E. D.; Westman, G.; Gray, D. G. Cationic surface functionalization of cellulose nanocrystals. *Soft Matter* **2008**, *4*, 2238–2244.
- (12) Espinosa, S. C.; Kuhnt, T.; Foster, E. J.; Weder, C. Isolation of Thermally Stable Cellulose Nanocrystals by Phosphoric Acid Hydrolysis. *Biomacromolecules* **2013**, *14*, 1223–1230.
- (13) Mao, J.; Osorio-Madrazo, A.; Laborie, M.-P. Preparation of cellulose I nanowhiskers with a mildly acidic aqueous ionic liquid: reaction efficiency and whiskers attributes. *Cellulose* **2013**, *20*, 1829–1840.
- (14) Mariano, M.; El Kissi, N.; Dufresne, A. Cellulose nanocrystals and related nanocomposites: Review of some properties and challenges. *J. Polym. Sci., Part B: Polym. Phys.* **2014**, *52*, 791–806.
- (15) Lin, N.; Huang, J.; Dufresne, A. Preparation, properties and applications of polysaccharide nanocrystals in advanced functional nanomaterials: A review. *Nanoscale* **2012**, *4*, 3274–3294.
- (16) Cetin, N. S.; Tingaut, P.; Ozmen, N.; Henry, N.; Harper, D.; Dadmun, M.; Sebe, G. Acetylation of Cellulose Nanowhiskers with Vinyl Acetate under Moderate Conditions. *Macromol. Biosci.* **2009**, *9*, 997–1003.
- (17) Nogi, M.; Abe, K.; Handa, K.; Nakatsubo, F.; Ifuku, S.; Yano, H. Property enhancement of optically transparent bionanofiber composites by acetylation. *Appl. Phys. Lett.* **2006**, *89*, 233123.
- (18) Gousse, C.; Chanzy, H.; Excoffier, G.; Soubeiran, L.; Fleury, E. Stable suspensions of partially silylated cellulose whiskers dispersed in organic solvents. *Polymer* **2002**, *43*, 2645–2651.
- (19) Habibi, Y.; Goffin, A. L.; Schiltz, N.; Duquesne, E.; Dubois, P.; Dufresne, A. Bionanocomposites based on poly(epsilon-caprolactone)-grafted cellulose nanocrystals by ring-opening polymerization. *J. Mater. Chem.* **2008**, *18*, 5002–5010.
- (20) Lin, N.; Chen, G. J.; Huang, J.; Dufresne, A.; Chang, P. R. Effects of Polymer-Grafted Natural Nanocrystals on the Structure and Mechanical Properties of Poly(lactic acid): A Case of Cellulose Whisker-graft-Polycaprolactone. *J. Appl. Polym. Sci.* **2009**, *113*, 3417–3425.
- (21) Zoppe, J. O.; Peresin, M. S.; Habibi, Y.; Venditti, R. A.; Rojas, O. J. Reinforcing Poly(epsilon-caprolactone) Nanofibers with Cellulose Nanocrystals. *ACS Appl. Mater. Interfaces* **2009**, *1*, 1996–2004.
- (22) Cranston, E. D.; Gray, D. G. Morphological and optical characterization of polyelectrolyte multilayers incorporating nanocrystalline cellulose. *Biomacromolecules* **2006**, *7*, 2522–2530.

- (23) Utsel, S.; Bruce, C.; Pettersson, T.; Fogelstrom, L.; Carlmark, A.; Malmstrom, E.; Wagberg, L. Physical Tuning of Cellulose-Polymer Interactions Utilizing Cationic Block Copolymers Based on PCL and Quaternized PDMAEMA. *ACS Appl. Mater. Interfaces* **2012**, *4*, 6796–6806.
- (24) Bondeson, D.; Oksman, K. Dispersion and characteristics of surfactant modified cellulose whiskers nanocomposites. *Compos. Interfaces* **2007**, *14*, 617–630.
- (25) Heux, L.; Chauve, G.; Bonini, C. Nonflocculating and chiral-nematic self-ordering of cellulose microcrystals suspensions in nonpolar solvents. *Langmuir* **2000**, *16*, 8210–8212.
- (26) Kvien, I.; Tanem, B. S.; Oksman, K. Characterization of cellulose whiskers and their nanocomposites by atomic force and electron microscopy. *Biomacromolecules* **2005**, *6*, 3160–3165.
- (27) Ljungberg, N.; Bonini, C.; Bortolussi, F.; Boisson, C.; Heux, L.; Cavaille, J. Y. New nanocomposite materials reinforced with cellulose whiskers in atactic polypropylene: Effect of surface and dispersion characteristics. *Biomacromolecules* **2005**, *6*, 2732–2739.
- (28) Petersson, L.; Kvien, I.; Oksman, K. Structure and thermal properties of poly(lactic acid)/cellulose whiskers nanocomposite materials. *Compos. Sci. Technol.* **2007**, *67*, 2535–2544.
- (29) Salajkova, M.; Berglund, L. A.; Zhou, Q. Hydrophobic cellulose nanocrystals modified with quaternary ammonium salts. *J. Mater. Chem.* **2012**, *22*, 19798–19805.
- (30) Fortunati, E.; Armentano, I.; Zhou, Q.; Iannoni, A.; Saino, E.; Visai, L.; Berglund, L. A.; Kenny, J. M. Multifunctional bionanocomposite films of poly(lactic acid), cellulose nanocrystals and silver nanoparticles. *Carbohydr. Polym.* **2012**, *87*, 1596–1605.
- (31) Agarwal, B. D.; Broutman, L. J. *Analysis and Performance of Fiber Composites*, 2nd ed.; Wiley: New York, 1990.
- (32) Halpin, J. C.; Kardos, J. L. The Halpin-Tsai Equations: A Review. *Polym. Eng. Sci.* **1976**, *16*, 344–352.
- (33) Diddens, I.; Murphy, B.; Krisch, M.; Muller, M. Anisotropic Elastic Properties of Cellulose Measured Using Inelastic X-ray Scattering. *Macromolecules* **2008**, *41*, 9755–9759.
- (34) Rusli, R.; Eichhorn, S. J. Determination of the stiffness of cellulose nanowhiskers and the fiber-matrix interface in a nanocomposite using Raman spectroscopy. *Appl. Phys. Lett.* **2008**, *93*, 033111.
- (35) Siqueira, G.; Bras, J.; Dufresne, A. New Process of Chemical Grafting of Cellulose Nanoparticles with a Long Chain Isocyanate. *Langmuir* **2010**, *26*, 402–411.
- (36) Saito, T.; Kimura, S.; Nishiyama, Y.; Isogai, A. Cellulose nanofibers prepared by TEMPO-mediated oxidation of native cellulose. *Biomacromolecules* **2007**, *8*, 2485–2491.
- (37) Alila, S.; Boufi, S.; Belgacem, M. N.; Beneventi, D. Adsorption of a cationic surfactant onto cellulosic fibers - I. Surface charge effects. *Langmuir* **2005**, *21*, 8106–8113.
- (38) Aloulou, F.; Boufi, S.; Belgacem, N.; Gandini, A. Adsorption of cationic surfactants and subsequent adsolubilization of organic compounds onto cellulose fibers. *Colloid Polym. Sci.* **2004**, *283*, 344–350.
- (39) Miyagi, Z.; Tanaka, K. Sorption of water vapor by poly(vinyl acetate). *Colloid Polym. Sci.* **1979**, *257*, 259–265.
- (40) Galperin, I.; Arheim, W. The Effect of Humidity on the Tensile Properties of TiO₂-Filled Poly(vinyl acetate). *J. Appl. Polym. Sci.* **1967**, *11*, 1259–1269.
- (41) Mathew, A. P.; Gong, G.; Björngrim, N.; Wixe, D.; Oksman, K. Moisture absorption behavior and its impact on the mechanical properties of cellulose whiskers-based polyvinylacetate nanocomposites. *Polym. Eng. Sci.* **2011**, *51*, 2136–2142.
- (42) Lindemann, M. K. Vinyl Acetate Polymers. In *Encyclopedia of Polymer Science And Technology*, Mark, H., Gaylord, N., Bikales, N., Eds.; Wiley-Interscience Publishers: New York, 1971; Vol. 15, p 577.
- (43) Delin, M.; Rychwalski, R. W.; Kubát, J.; Klason, C.; Hutchinson, J. M. Physical aging time scales and rates for poly(vinyl acetate) stimulated mechanically in the Tg-region. *Polym. Eng. Sci.* **1996**, *36*, 2955–2967.
- (44) Kobayashi, Y.; Zheng, W.; Meyer, E. F.; McGervey, J. D.; Jamieson, A. M.; Simha, R. Free volume and physical aging of poly(vinyl acetate) studied by positron annihilation. *Macromolecules* **1989**, *22*, 2302–2306.
- (45) Keddie, J. L.; Jones, R. A. L.; Cory, R. A. Interface and Surface Effects on the Glass-Transition Temperature in Thin Polymer-Films. *Faraday Discuss.* **1994**, *98*, 219–230.
- (46) Henriksson, M.; Fogelström, L.; Berglund, L. A.; Johansson, M.; Hult, A. Novel nanocomposite concept based on cross-linking of hyperbranched polymers in reactive cellulose nanopaper templates. *Compos. Sci. Technol.* **2011**, *71*, 13–17.
- (47) Ansari, F.; Galland, S.; Johansson, M.; Plummer, C. J. G.; Berglund, L. A. Cellulose nanofiber network for moisture stable, strong and ductile biocomposites and increased epoxy curing rate. *Composites, Part A* **2014**, *63*, 35–44.
- (48) Ansari, F.; Skrifvars, M.; Berglund, L. Nanostructured biocomposites based on unsaturated polyester resin and a cellulose nanofiber network. *Compos. Sci. Technol.* **2015**, *117*, 298–306.
- (49) Strum, L. C. E. Physical Aging in Plastics and Other Glassy Materials. *Polym. Eng. Sci.* **1977**, *17*, 165–173.
- (50) Boucher, V. M.; Cangialosi, D.; Alegria, A.; Colmenero, J. Time dependence of the segmental relaxation time of poly(vinyl acetate)-silica nanocomposites. *Phys. Rev. E* **2012**, *86*, 041501.
- (51) Cangialosi, D.; Boucher, V. M.; Alegria, A.; Colmenero, J. Physical aging in polymers and polymer nanocomposites: recent results and open questions. *Soft Matter* **2013**, *9*, 8619.
- (52) Cangialosi, D.; Boucher, V. M.; Alegria, A.; Colmenero, J. Enhanced physical aging of polymer nanocomposites: The key role of the area to volume ratio. *Polymer* **2012**, *53*, 1362–1372.
- (53) Barroso-Bujans, F.; Boucher, V. M.; Pomposo, J. A.; Buruaga, L.; Alegria, A.; Colmenero, J. Easy-dispersible poly(glycidyl phenyl ether)-functionalized graphene sheets obtained by reaction of "living" anionic polymer chains. *Chem. Commun. (Cambridge, U. K.)* **2012**, *48*, 2618–20.
- (54) Gong, G.; Pyo, J.; Mathew, A. P.; Oksman, K. Tensile behavior, morphology and viscoelastic analysis of cellulose nanofiber-reinforced (CNF) polyvinyl acetate (PVAc). *Composites, Part A* **2011**, *42*, 1275–1282.
- (55) Gong, G.; Mathew, A. P.; Oksman, K. Toughening effect of cellulose nanowhiskers on polyvinyl acetate: Fracture toughness and viscoelastic analysis. *Polym. Compos.* **2011**, *32*, 1492–1498.
- (56) Sapkota, J.; Kumar, S.; Weder, C.; Foster, E. J. Influence of Processing Conditions on Properties of Poly (Vinyl acetate)/Cellulose Nanocrystal Nanocomposites. *Macromol. Mater. Eng.* **2015**, *300*, 562–571.
- (57) Eriksson, M.; Goossens, H.; Peijs, T. Influence of drying procedure on glass transition temperature of PMMA based nanocomposites. *Nanocomposites* **2015**, *1*, 36–45.